Electronic Supplementary Material (ESI) for Nanoscale.

Facile modular approach to 2D oriented assembly MOFs electrode for non-enzymatic sweat biosensor

Zhengyun Wang, Mengxi Gui, Muhammad Asif, Yang Yu, Shuang Dong, Haitao Wang, Wei Wang, Feng Wang, Fei Xiao and Hongfang Liu*

Key Laboratory of Material Chemistry for Energy Conversion and Storage, Ministry of Education, Hubei Key Laboratory of Material Chemistry and Service Failure, School of Chemistry and Chemical Engineering, Huazhong University of Science and Technology, Wuhan 430074, P. R. China.

Table of Contents

1. Details about electrode preparation

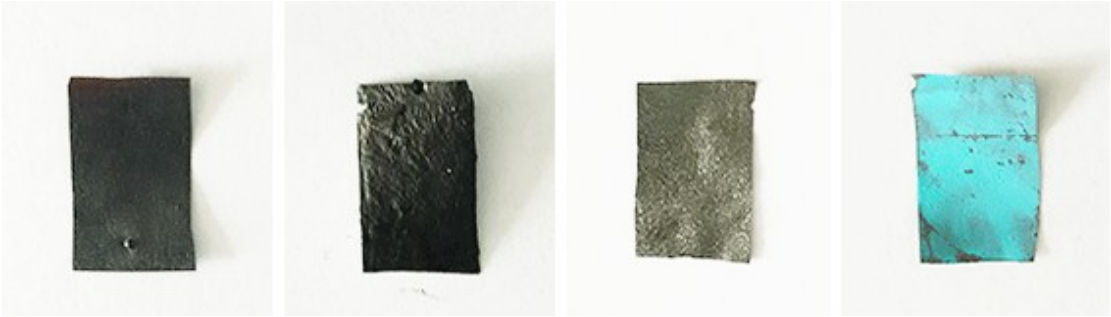

Figure S1 photographs of GOP, NH_2-GOP, NH_2-GP and **NH_2-GP-$Cu_3(btc)_2$** (From left to right)

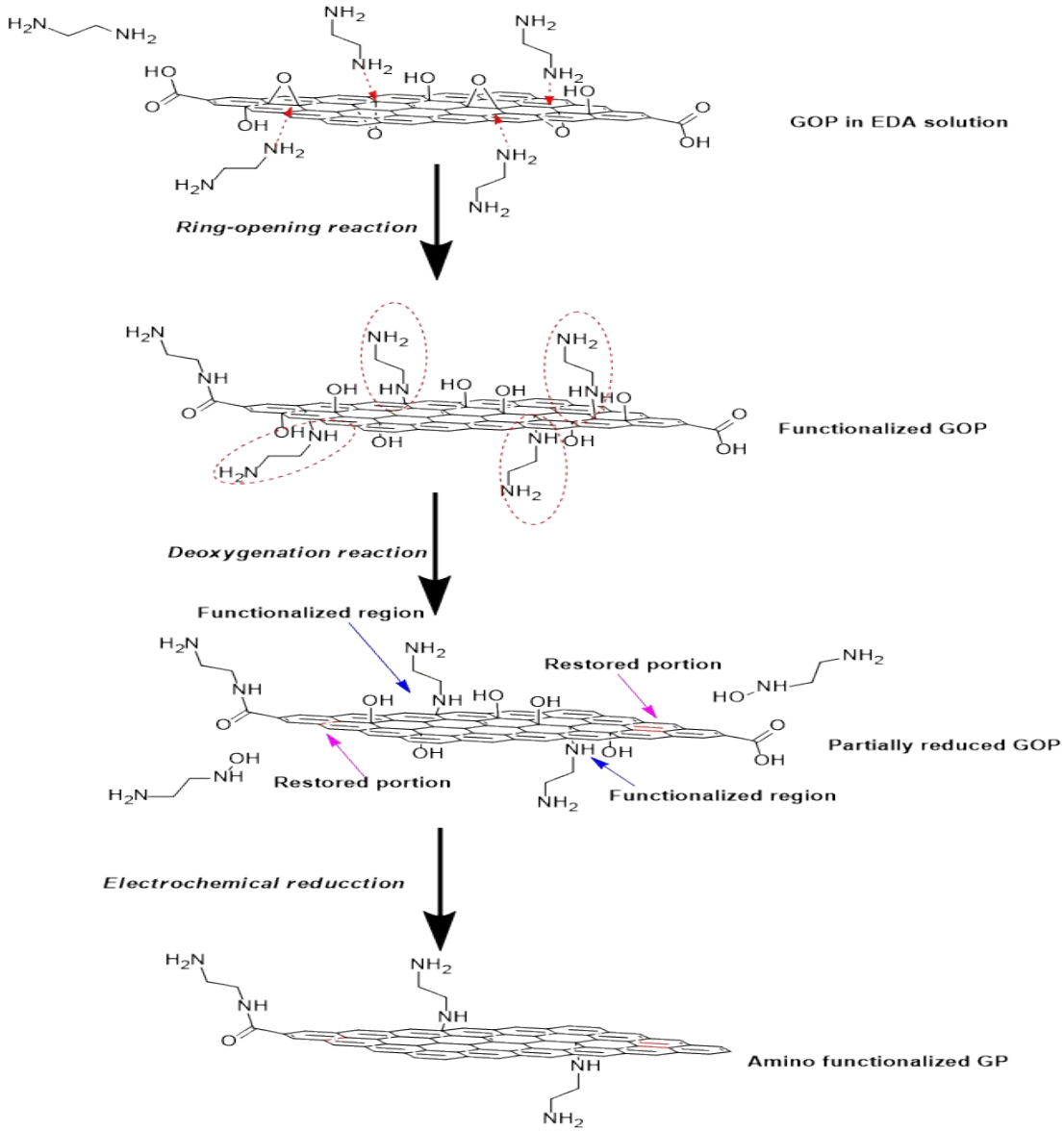

Figure S2 Schematic formation NH_2-GOP and NH_2-GP

2. Details about 2D-assembly of $Cu_3(btc)_2$ nanocubes

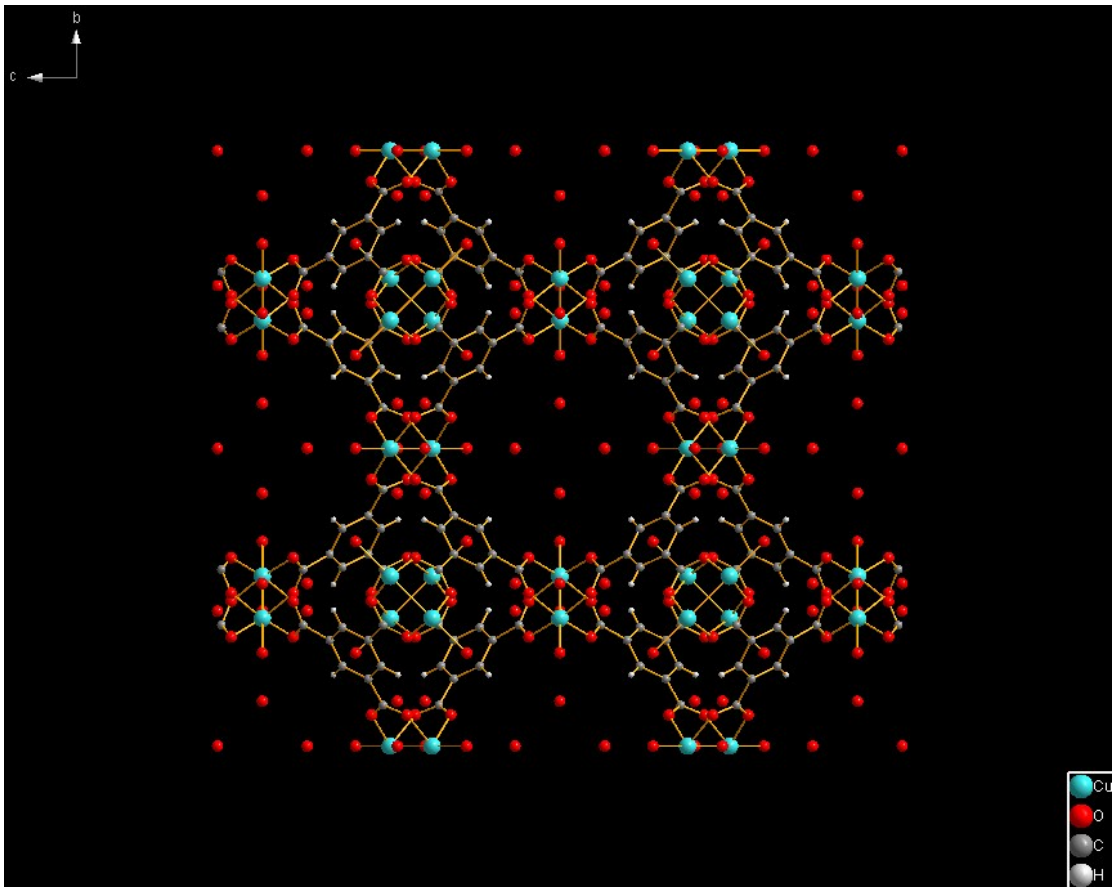

Figure S3 The schematic crystal structures of the $Cu_3(btc)_2$ viewed by {100} crystal plane.

The results of zeta potential test showed that $Cu_3(btc)_2$ nanocubes were negatively charged because of oxygen groups and NH_2-GP was positively charged due to amino groups. Interfacial reaction time control is very important to prepare the $Cu_3(btc)_2$ nanocubes. If the time of interfacial reaction for the preparation $Cu_3(btc)_2$ is too long (more than 1 min), after demulsification, the obtained morphologies are irregular, as shown in Figure S4A and Figure S4B. If the time is too short (less than 5 s), the obtained morphologies are not nanocubes, as shown in Figure S4C and Figure S4D. The suitable time to obtain nanocubes is around 12 s.

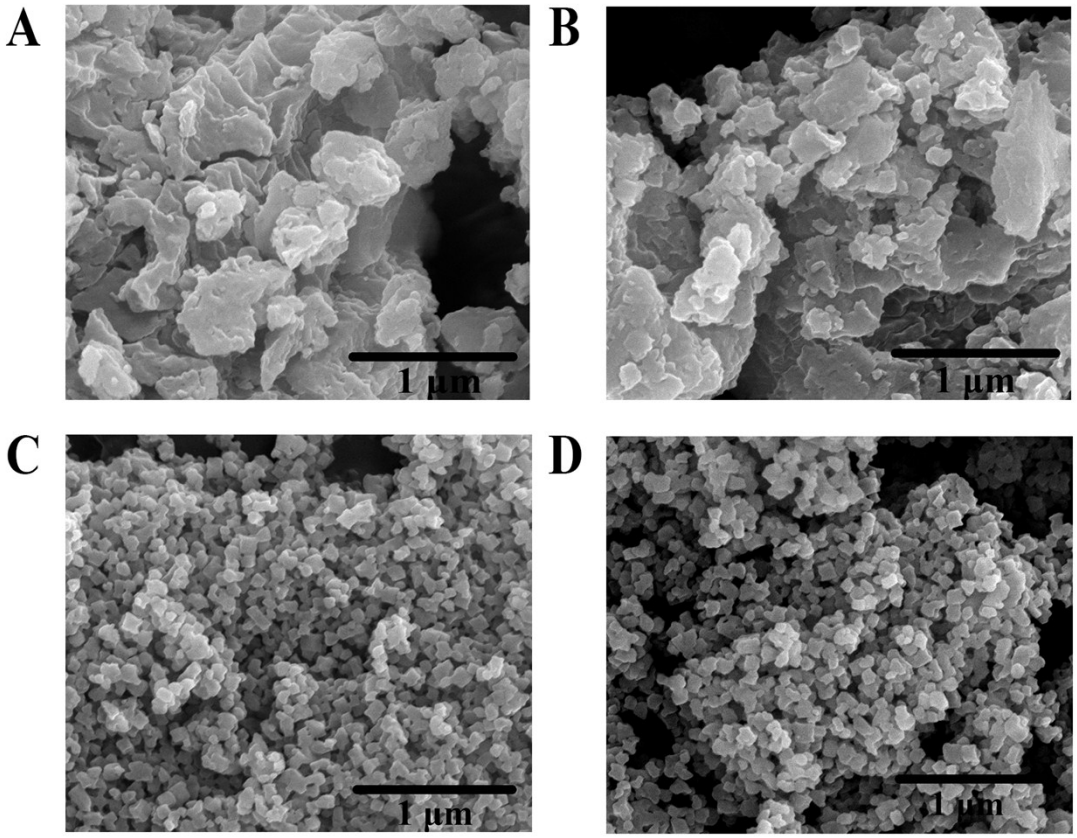

Figure S4 (A) and (B) $Cu_3(btc)_2$ with interfacial reaction for 2 min (C) and (D) $Cu_3(btc)_2$ with interfacial reaction for 5 s

$Cu_3(btc)_2$ nanocubes stayed in the interfaces and formed a blue layer. NH_2-GP was immersed into the water phase and moved towards the blue layer to finish dip-coating.

3. EIS and CV

Since the bare $Cu_3(btc)_2$ is powder materials, the EIS and CV tests of $Cu_3(btc)_2$ need the use of glass carbon electrode. The preparation is as followings: Glassy carbon electrode was polished with emery paper and alumina slurry; they were then successively rinsed with dilute nitric acid, ethanol, and distilled water in an ultrasonic bath. Thereafter, the electrode was immersed in 0.25 M H_2SO_4 and the potential at the electrode were changed in the -1.0 and 1.0 V range until a steady potential was obtained. $Cu_3(btc)_2$ nanocubes were dispersed in ethanol (approximately 1.0

mg/mL solution). Then 15 μL of this suspension was deposited on the surface of the GCE. The solvent was allowed to evaporate to dryness in air and the $Cu_3(btc)_2$ nanocubes formed very stable films.

The interfacial properties of surface-modified electrodes have been characterized by EIS. EIS experiments were performed with CHI760E electrochemical workstation (CH Instrument Company, Shanghai, China). A conventional three-electrode system was adopted. The working electrode was a contacted material, and the auxiliary and reference electrodes were Pt foil and saturated calomel electrode (SCE), respectively. The Nyquist plots of GOP, NH_2-GOP, NH_2-GP, $Cu_3(btc)_2$ and **NH_2-GP-$Cu_3(btc)_2$** electrode was tested in 0.6 M NaCl containing 1.0 mM $K_3Fe(CN)_6$ and 1.0 mM $K_4Fe(CN)_6$. The volume of electrolyte is 6 mL. The frequency range is 0.1–10^5 Hz.

The CV of $Cu_3(btc)_2$ is also tested. The bare $Cu_3(btc)_2$ has weak sensing performances toward lactate. The current response increases with the increased concentration of lactate. The NH_2-GP with excellent conductivity can improve the sensing performances.

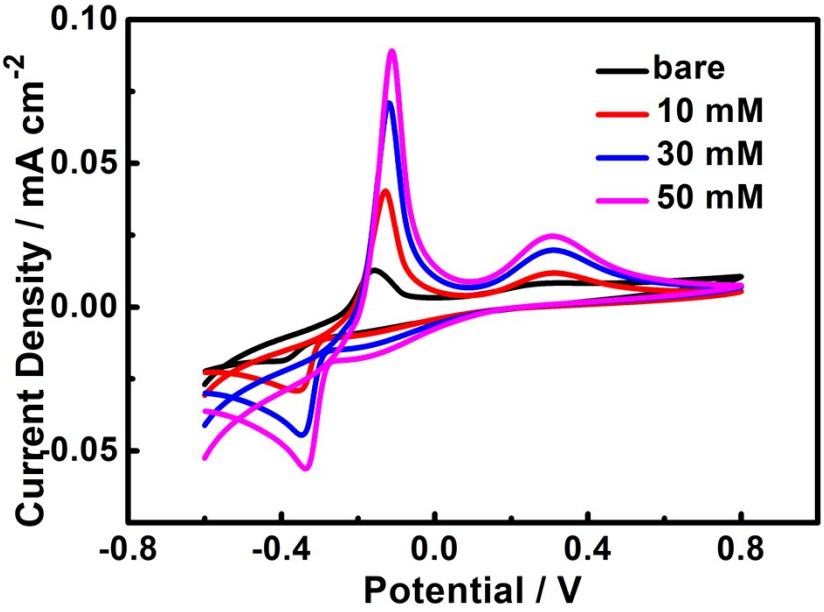

Figure S5 CV programs of bare $Cu_3(btc)_2$ in PBS (containing 0.6 M NaCl) in the absence and presence of lactate with different concentrations (10 mM-50 mM).

Also, The effect of different scan rates at **NH_2-GP-$Cu_3(btc)_2$** with lactate and glucose were also investigated. The CVs of the **NH_2-GP-$Cu_3(btc)_2$** in PBS (pH=8.0) were collected with different scan rates from 10 mV/s to 200 mV/s, and the peak currents increased linearly with the square root of the scan rate. It would appear that diffusion controlled process could be responsible for lactate and glucose oxidation.

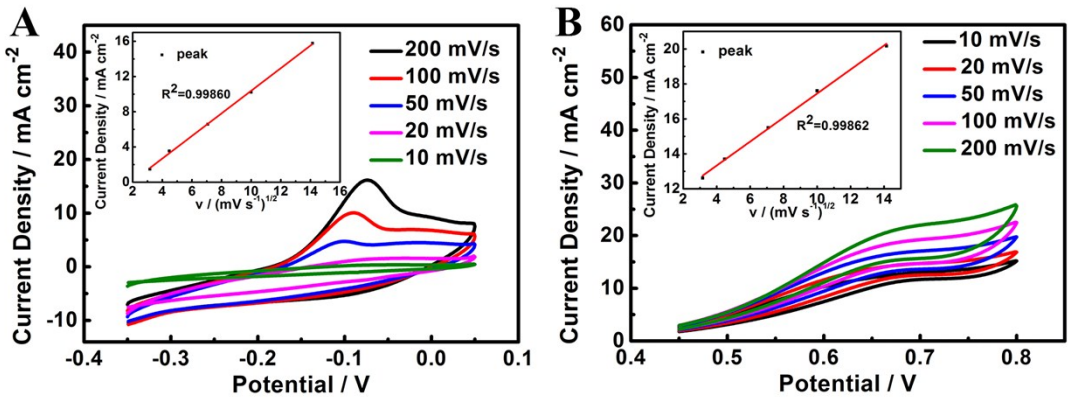

Figure S6 CVs of **NH_2-GP-$Cu_3(btc)_2$** 0.1 M PBS with 0.6 M NaCl with (A) 10 mM

lactate and (B) 1 mM glucose (pH = 8.0) at different scan rates from 10 to 200 mV/s. Inset is plot of peak current versus the square root of the scan rate.

4. Optimization of conditions for lactate detection

Ionic strength

Interestingly, the increase of ionic strength will enlarge the current response toward lactate. Considering that a great quantity of inorganic salts is rich in human perspiration, especially NaCl, thus PBS with a high ionic strength (NaCl) is used as electrolyte to test the hybrid electrode. The concentration of NaCl is optimized. The PBS solution with 0.6 M NaCl is chosen for the test due to the highest response.

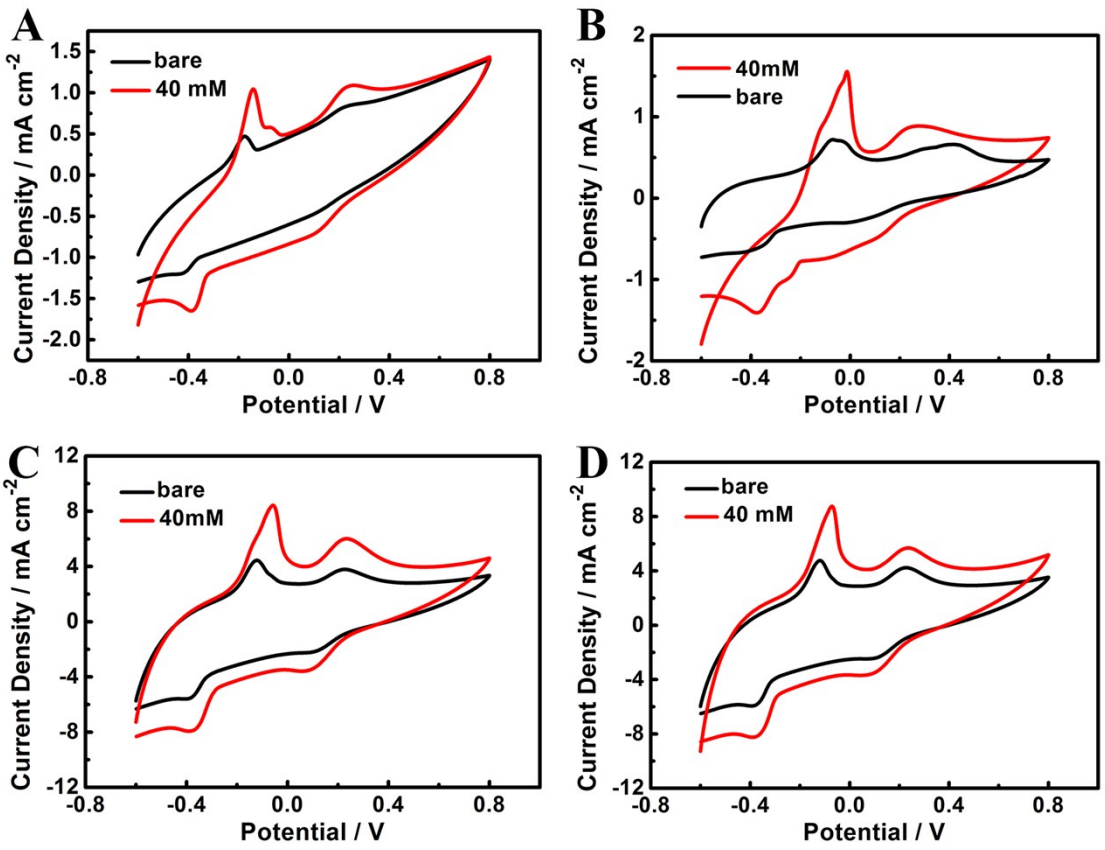

Figure S7 (A)-(D) Cyclic voltammogram of **NH_2-GP-$Cu_3(btc)_2$** electrode in PBS (pH = 8.0) solution with various concentration of NaCl (0.2, 0.4, 0.5 and 0.6 M for A, B, C, D, respectively) in the absence (black line) and presence (red line) of 40 mM

lactate. Scan rate: 50 mV/s

Working potential

The effect of working potential on the performance of the **NH_2-GP-$Cu_3(btc)_2$** was investigated in the detection solution containing 0.8 mM lactate. From Figure S8, the **NH_2-GP-$Cu_3(btc)_2$** showed a maximum current change of 0.8 mM lactate at potential of -0.1 V. Consequently, an operational potential value of -0.1 V, was chosen for subsequent amperometric measurements for lactate.

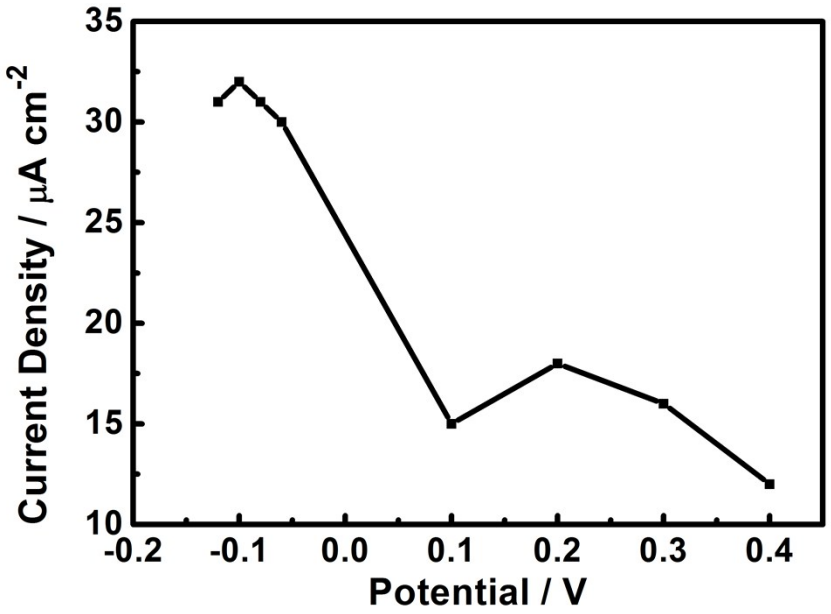

Figure S8 The influence of different working potentials on **NH_2-GP-$Cu_3(btc)_2$** biosensor response to 0.8 mM lactate.

Temperature

The great influence from the temperature should be considered. Since our electrode is used in general terms, we chose the temperature from 18 ℃ to 38 ℃， to compare and optimize. The results showed that the temperature had little effect on catalytic activity in such a relatively mild temperature range.

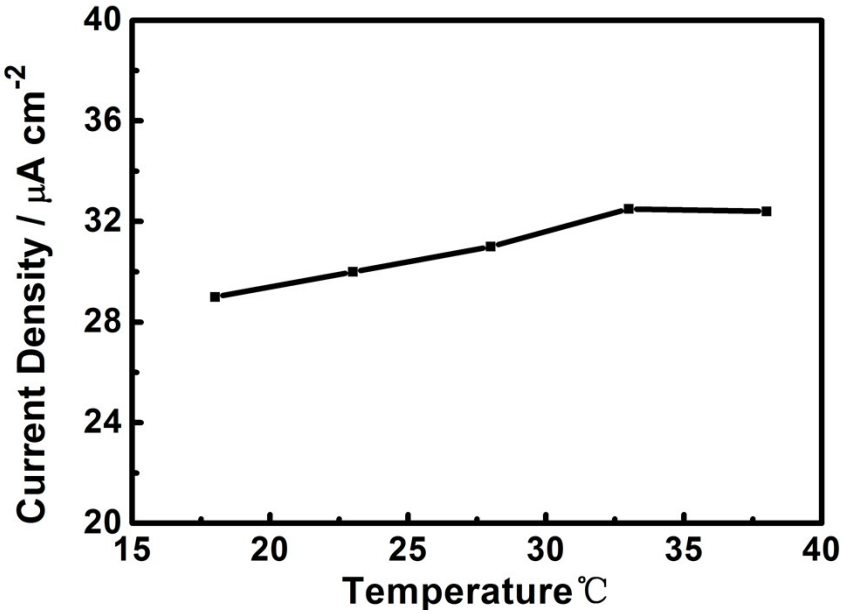

Figure S9 The influence of different temperatures on **NH_2-GP-$Cu_3(btc)_2$** biosensor response to 0.8 mM lactate.

pH

We chose the pH as 7.6, 7.8, 8.2, 8.2, respectively, to compare and optimize. The results showed that catalytic activity for lactate sensing reached the highest when the pH equals to 8.0.

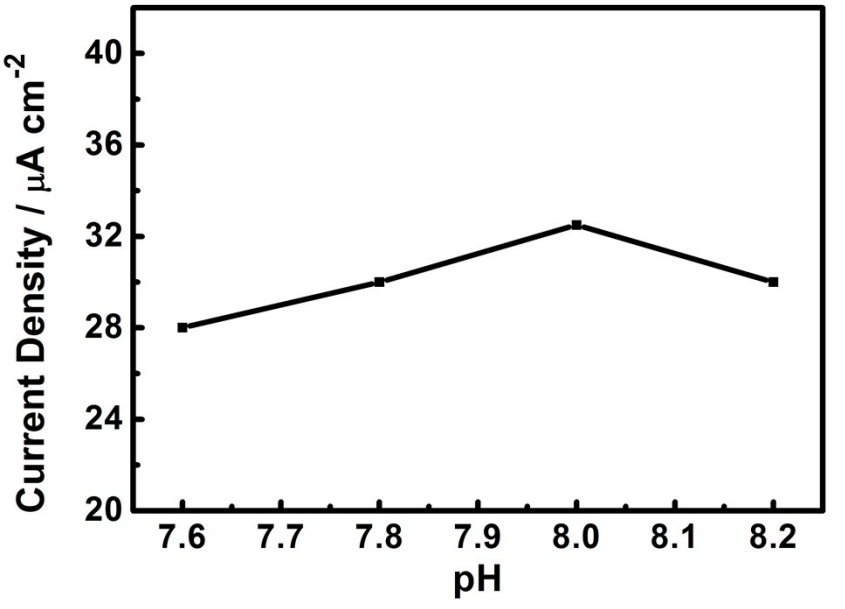

Figure S10 The influence of different pH on **NH_2-GP-$Cu_3(btc)_2$** biosensor response to

0.8 mM lactate.

5. Optimization of conditions for glucose detection

Ionic strength

The Cu(II)/Cu(III) redox couple, which has been reported to be strongly dependent upon the hydroxide concentration, was considered playing an important role for glucose oxidation. For glucose sensing, sodium ions tend to occupy the nanopores of MOFs, thereby preventing the entry of hydroxyl and leading decreasing of current response. But the sensing performance for glucose is still excellent. We still chose the PBS solution (pH=8.0) with 0.6 M NaCl as the electrolyte since this concentration is more beneficial to lactate sensing.

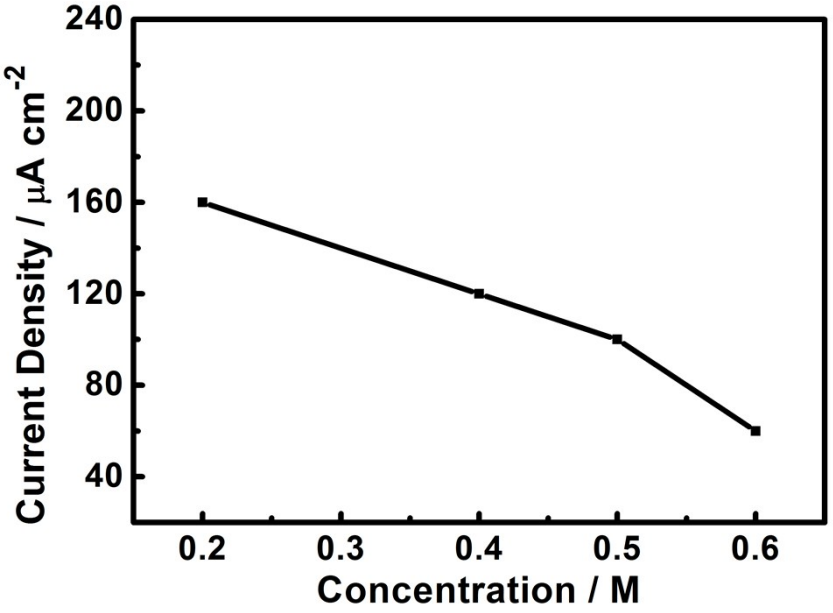

Figure S11 Response of **NH_2-GP-$Cu_3(btc)_2$** electrode toward 300 nM glucose in PBS (pH = 8.0) solution with various concentration of NaCl from 0.2 M to 0.6 M.

Working potential

The dependence of the **NH_2-GP-$Cu_3(btc)_2$** biosensor response on the applied potential was evaluated over the potential range from 0.55 V to 0.75 V for glucose in

PBS solution. The **NH_2-GP-$Cu_3(btc)_2$** showed a maximum current change of 300 nM glucose at potential of +0.65 V. Consequently, an operational potential value of +0.65 V was chosen for subsequent amperometric measurements for glucose.

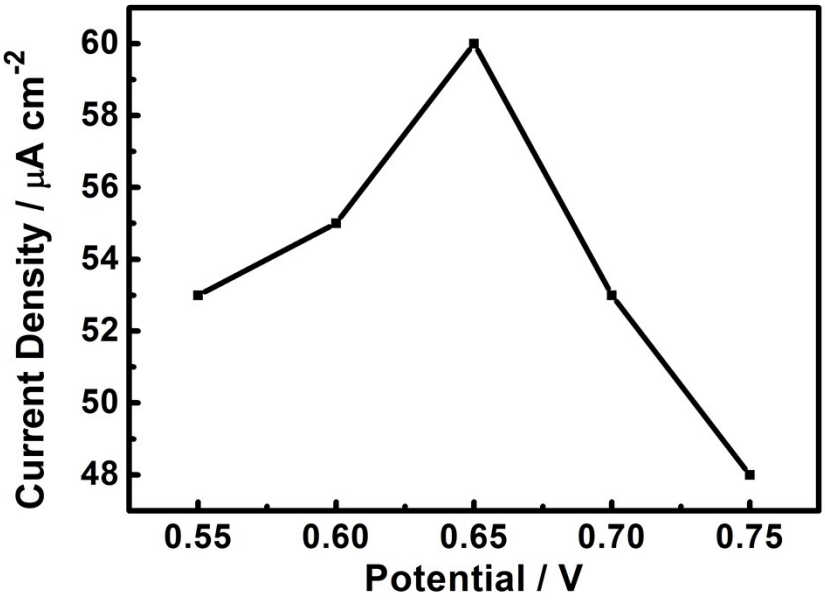

Figure S12 The influence of different potentials on **NH_2-GP-$Cu_3(btc)_2$** biosensor response to 300 nM glucose.

Temperature

We chose the temperature from 18 ℃ to 38 ℃ to compare and optimize. The results showed that the temperature had little effect on catalytic activity for glucose sensing in such a relatively mild temperature range.

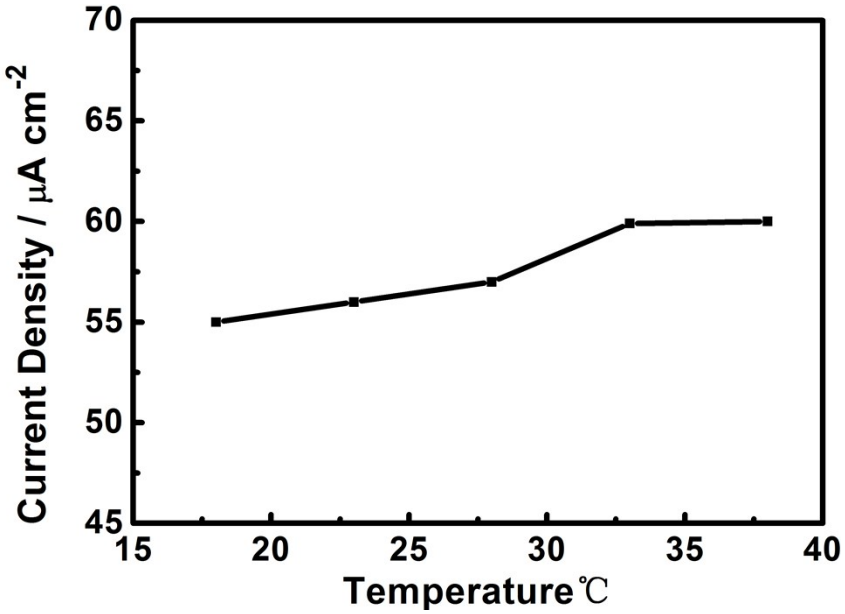

Figure S13 The influence of different temperatures on **NH_2-GP-$Cu_3(btc)_2$** biosensor response to 300 nM glucose.

pH

We chose the wide pH to compare and optimize. The results showed that catalytic activity for glucose sensing reaches the highest when the pH equals to 13. But considering that the strong alkali solution is not suitable for wearable sensors and the effects of pH, the PBS (pH=8.0) was chosen for glucose sensing.

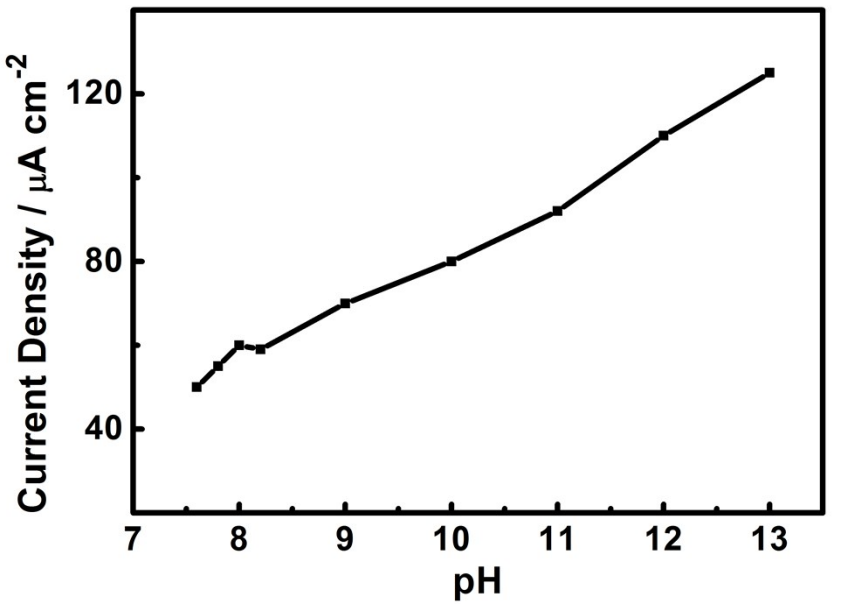

Figure S14 The influence of different pH on **NH_2-GP-Cu_3(btc)$_2$** biosensor response to 300 nM glucose.

6. Current response comparison between NH_2-GP and NH_2-GP-Cu_3(btc)$_2$

The current responses of NH_2-GP and **NH_2-GP-Cu_3(btc)$_2$** electrode toward glucose and lactate were evaluated. The results showed that NH_2-GP has no response to glucose and lactate.

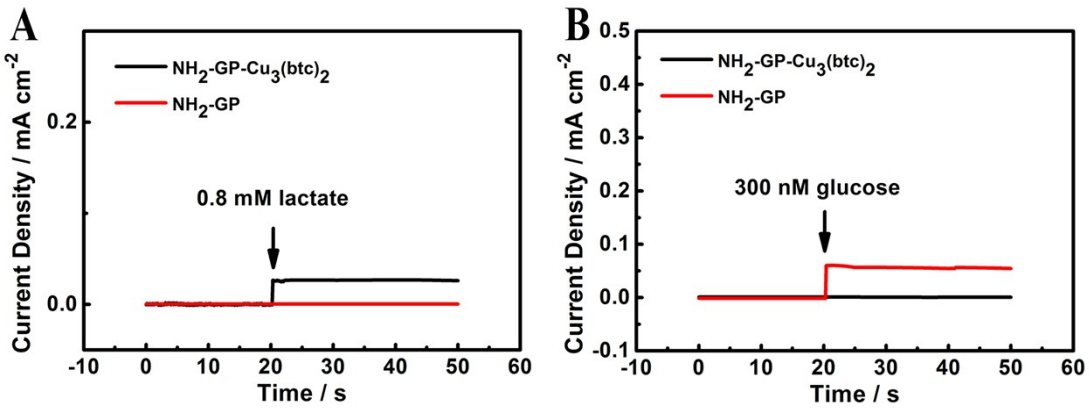

Figure S15 (A) Current response of **NH_2-GP-Cu_3(btc)$_2$** and NH_2-GP toward 0.8 mM lactate (B) Current response of **NH_2-GP-Cu_3(btc)$_2$** and NH_2-GP to 300 nM glucose.

7. Recycling property

When **NH_2-GP-Cu_3(btc)$_2$** biosensor was full deactivate after a long time, the NH_2-GP can be reused to assemble the new Cu_3(btc)$_2$ nanocubes. The results show that the electrochemical performances for detection of glucose and lactate can be recovered and reaches to the initial state, demonstrating the NH_2-GP can be easy-recycled.

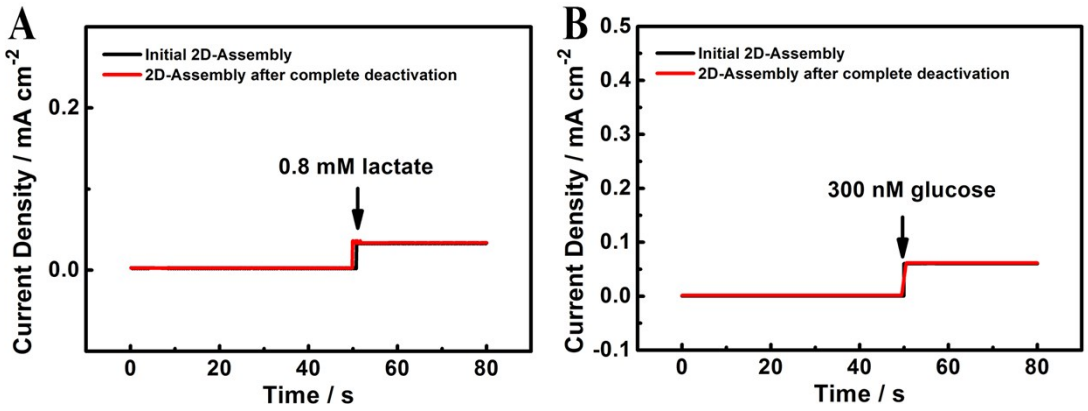

Figure S16 (A) Current response of **NH_2-GP-Cu_3(btc)$_2$** and twice 2D-assmbly after complete deactivation toward 0.8 mM lactate (B) Current response of **NH_2-GP-Cu_3(btc)$_2$** and twice 2D-assmbly after complete deactivation toward to 300 nM glucose.

8. Sensing performances of reported analogue electrochemical biosensors

Table S1

Electrode for glucose	Sensitivity ($mAcm^{-2}mM^{-1}$)	Detection Limit(μM)	Linear Range(mM)	Ref
NH_2-GP-Cu_3(btc)$_2$	5.36	0.03	0.00005-1.7755	This work
Cu-Graphene	-	0.5	Up to 4.5	1
PEDOT/GO	0.9091	0.047	0.0001-1.3	2
rGO/Co_3O_4	3.39	<25	-	3
PdCuPt	0.378	1.29	1-10	4
AuNP/NG	-	12	0.04-16.1	5
Electrode for lactate	Sensitivity ($\mu Acm^{-2}mM^{-1}$)	Detection Limit(μM)	Linear Range(mM)	Ref
NH_2-GP-Cu_3(btc)$_2$	29	5	0.05-22.6	This work
PVI-OS/CNT-LOD	-	0.6	-	6
Pt-nafion-LOD	-	0.8	0.002-1	7
Pt/PDDA-CMM-LOD	-	<5	-	8
N-CNT-LOD	4	4.1	0.014-0.325	9
PtNps/GCNF-LOD	4.13	6.9	-	10

9. Procedures of sweat test and ultraviolet spectrophotometry correlating and validating

Procedures of sweat test

The perspiration sample was sampled from a healthy male volunteer with no prior medical history of heart conditions, diabetes or chronic skeletomuscular pain who exercised for three hours before test. Exercise includes basketball, running and instrument training. Due to long time and high intensity for exercise, the transfer liquid gun was used to collect a large amount of sweat (6.5 mL). The volume and pH of sweat for electrochemical test are 0.5 mL and 6.7, respectively. The volume and pH of the electrolyte are 6 mL and 8.0, respectively. Before dynamic measurement, we test the bare PBS for static blank. Amperometric measurements were carried out with twin-channel electrochemical workstation at applied potential of -0.1 V for lactate analysis and +0.65 V for glucose analysis by **NH_2-GP-$Cu_3(btc)_2$**. Electrochemical workstation within two working channels ensures simultaneous detection. After dynamic measurement, we used the same system to continue the static response test for comparing.

Ultraviolet spectrophotometry correlating and validating

In order to correlate and validate our developed method, we chose the typical and classical ultraviolet spectrophotometry method to calibrate. In a strong acid solution, glucose will dehydrate and hydroxymethyl furfural will be produced. The position of maximum absorption for hydroxymethyl furfural is at the wavelength of 286 nm and lactate has no effects at this wavelength. Specific procedures are as follows:

(1) 1 mM glucose standard solution was accurately measured and put in a test tube with 3 mL Hydrochloric acid. The tube was filled up to 6 mL with distilled water.

And then, it was heated in boiling water for 8min. After cooling down to the room temperature, proper amount of solution was taken to scan with Spectrumlab from 200 nm to 400 nm. Its ultraviolet maximum absorption wavelength was determined as 286 nm.

(2) 0.005 mM, 0.05 mM, 0.2 mM, 1 mM, 1.8 mM glucose standard solutions were precisely measured to test for standard curve. The absorbance was measured at 286 nm by using blank as reference. There was a good linear relationship between glucose concentration and absorbance (0.005-1.8 mM),

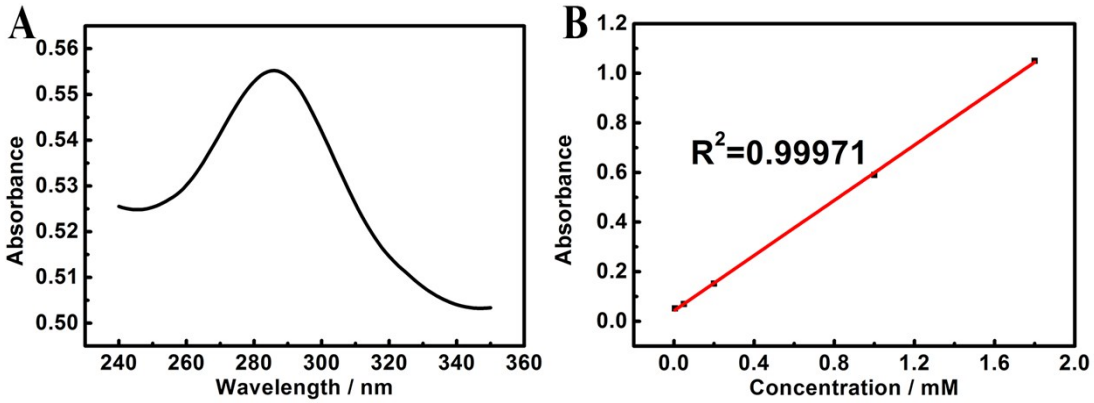

Figure S17 (A) Absorbance spectra of hydroxymethyl furfural (B) Linear relationship between absorbance and glucose concentration.

Similarly, the position of maximum absorption for lactate is at the wavelength of 210 nm and glucose has no effects at this wavelength. Specific procedures are as follows:

(1) 0.005 mM lactate standard solution was accurately measured and put in a test tube. The tube was filled up to 6 mL with distilled water. Proper amount of solution was taken to scan with Spectrumlab from 200 nm to 300 nm. Its ultraviolet maximum absorption wavelength was determined as 210 nm. (Figure S18A)

(2) 0.01 mM, 0.1 mM, 1.0 mM, 10 mM, 20 mM lactate standard solutions were precisely measured to test for standard curve. The absorbance was measured at 210 nm by using blank as reference. There was a good linear relationship between lactate concentration and absorbance (0.01-20 mM), as shown in Figure S18B.

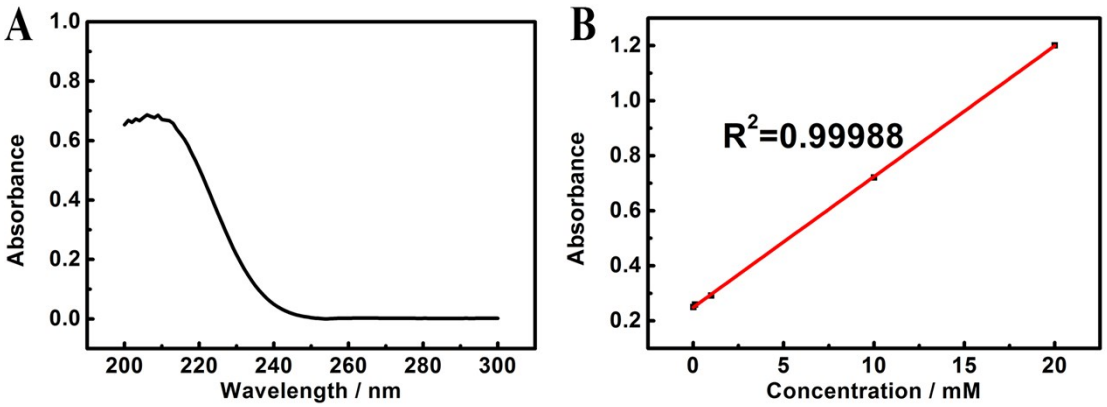

Figure S18 (A) Absorbance spectra of lactate (B) Linear relationship between absorbance and lactate concentration.

Table. S2 Linear equations, linear range and limits of quantization of UV test

Ingredient	linear equation	Linear range (mM)	Detection limit(μM)
lactate	**A=0.04751n+0.24897**	**0.01-20**	**2.0**
glucose	**A=0.5566n+0.03886**	**0.005-1.8**	**1.5**

As shown in Figure S19, the same perspiration was tested. The absorbance of sweat glucose and lactate were 0.322 and 0.704, respectively. According to the good linear aquation, the sweat glucose and lactate were estimated as 0.51 mM and 9.59 mM, respectively. Our results via electrochemical readouts are 0.52 mM and 9.80 mM, respectively, close to the results through Ultraviolet Spectrophotometry. The relative errors are 1.96% and 2.19%, respectively. These results demonstrate that our

electrochemical analysis to sweat glucose and lactate is credible.

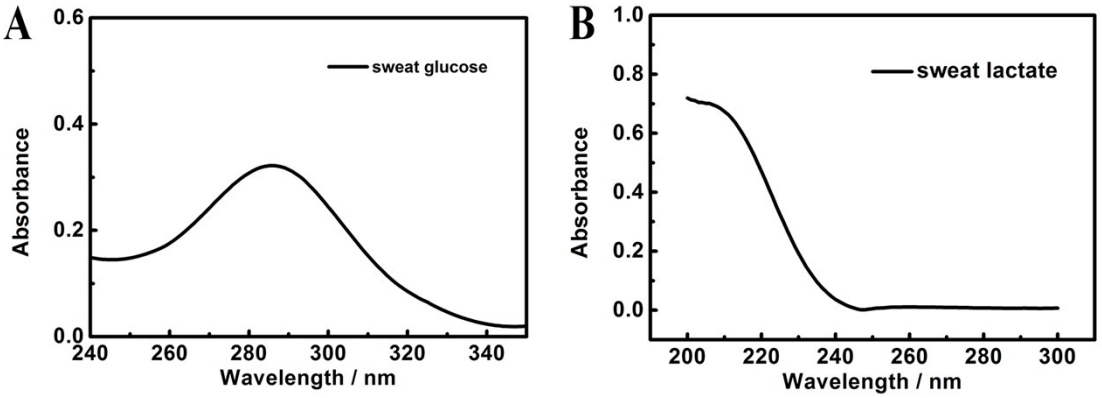

Figure S19 (A) Absorbance spectra of sweat glucose (B) Absorbance spectra of sweat lactate

10. References

1. J. Luo, S. Jiang, H. Zhang, J. Jiang and X. Liu, *Anal. Chim. Acta*, 2012, **709**, 47-53.
2. N. Hui, W. Wang, G. Xua and X. Luo, *Journal of Materials Chemistry B*, 2015, **3**, 556-561.
3. X.-C. Dong, H. Xu, X.-W. Wang, Y.-X. Huang, M. B. Chan-Park, H. Zhang, L.-H. Wang, W. Huang and P. Chen, *ACS Nano*, 2012, **6**, 3206-3213.
4. S. Fu, C. Zhu, J. Song, M. Engelhard, H. Xia, D. Du and Y. Lin, *Acs Applied Materials & Interfaces*, 2016, **8**, 22196-22200.
5. T. Tran Duy, J. Balamurugan, S. H. Lee, N. H. Kim and J. H. Lee, *Biosensors & Bioelectronics*, 2016, **81**, 259-267.
6. X. Li, J. Zang, Y. Liu, Z. Lu, Q. Li and C. M. Li, *Anal. Chim. Acta*, 2013, **771**, 102-107.
7. M. Ricardo Romero, F. Ahumada, F. Garay and A. M. Baruzzi, *Analytical*

Chemistry, 2010, **82**, 5568-5572.

8. Y. Yu, Y. Yang, H. Gu, T. Zhou and G. Shi, *Biosensors & Bioelectronics*, 2013, **41**, 511-518.

9. J. M. Goran, J. L. Lyon and K. J. Stevenson, *Analytical Chemistry*, 2011, **83**, 8123-8129.

10. O. A. Loaiza, P. J. Lamas-Ardisana, L. Anorga, E. Jubete, V. Ruiz, M. Borghei, G. Cabanero and H. J. Grande, *Bioelectrochemistry*, 2015, **101**, 58-65.